Constraining cloud lifetime effects of aerosols using A-Train satellite observations

Minghuai Wang,[1] Steven Ghan,[1] Xiaohong Liu,[1] Tristan S. L'Ecuyer,[2] Kai Zhang,[1] Hugh Morrison,[3] Mikhail Ovchinnikov,[1] Richard Easter,[1] Roger Marchand,[4] Duli Chand,[1] Yun Qian,[1] and Joyce E. Penner[5]

Received 30 April 2012; revised 3 July 2012; accepted 11 July 2012; published 15 August 2012.

[1] Aerosol indirect effects have remained the largest uncertainty in estimates of the radiative forcing of past and future climate change. Observational constraints on cloud lifetime effects are particularly challenging since it is difficult to separate aerosol effects from meteorological influences. Here we use three global climate models, including a multi-scale aerosol-climate model PNNL-MMF, to show that the dependence of the probability of precipitation on aerosol loading, termed the precipitation frequency susceptibility (S_{pop}), is a good measure of the liquid water path response to aerosol perturbation (λ), as both S_{pop} and λ strongly depend on the magnitude of autoconversion, a model representation of precipitation formation via collisions among cloud droplets. This provides a method to use satellite observations to constrain cloud lifetime effects in global climate models. S_{pop} in marine clouds estimated from CloudSat, MODIS and AMSR-E observations is substantially lower than that from global climate models and suggests a liquid water path increase of less than 5% from doubled cloud condensation nuclei concentrations. This implies a substantially smaller impact on shortwave cloud radiative forcing over ocean due to aerosol indirect effects than simulated by current global climate models (a reduction by one-third for one of the conventional aerosol-climate models). Further work is needed to quantify the uncertainties in satellite-derived estimates of S_{pop} and to examine S_{pop} in high-resolution models. **Citation:** Wang, M., et al. (2012), Constraining cloud lifetime effects of aerosols using A-Train satellite observations, *Geophys. Res. Lett.*, *39*, L15709, doi:10.1029/2012GL052204.

1. Introduction

[2] The indirect effects of aerosols on the planetary energy balance through their role in cloud droplet formation and cloud evolution involve two principal pathways. Aerosols influence cloud microphysical structure by modifying the size and optical properties of cloud droplets in what is often termed the cloud albedo effect. They can also lead to changes in cloud liquid water path (LWP) and cloud fraction, collectively known as cloud lifetime effects. Satellite observations have been used to constrain cloud albedo effects in climate models and typically produce smaller aerosol indirect forcing than solely model-based estimates [e.g., *Lohmann and Lesins*, 2002; *Quaas and Boucher*, 2005; *Quaas et al.*, 2008]. However, satellite approaches suffer from their own limitations, such as retrieval contamination of aerosol optical depth by clouds [*Marshak et al.*, 2006], and the impact of data aggregation [*McComiskey and Feingold*, 2012]. Another limitation of satellite approaches is that spatial variations in aerosol-cloud relationships derived from satellite observations do not necessarily represent the cloud response to aerosol perturbations from pre-industrial (PI) to present day (PD) conditions [*Penner et al.*, 2011].

[3] While determination of the albedo effect is difficult, it is even more challenging to use satellite observations to constrain cloud lifetime effects in climate models. Since LWP and cloud fraction are primarily determined by meteorological conditions rather than cloud microphysics [*Kubar et al.*, 2009], relationships between LWP/cloud fraction and aerosol loading can be elusive.

[4] The CloudSat satellite, along with other satellites in the A-Train constellation [*L'Ecuyer and Jiang*, 2010; *Stephens et al.*, 2002] provide nearly coincident high-resolution global observations of precipitation, aerosols and clouds, which allows the opportunity for a major advance in satellite studies of cloud lifetime effects. The synergistic use of these data has led to new insights into aerosol-cloud-precipitation interactions [e.g., *Kubar et al.*, 2009; *L'Ecuyer et al.*, 2009; *Leon et al.*, 2008; *Sorooshian et al.*, 2009; *Stephens and Haynes*, 2007; *Suzuki et al.*, 2010]. Here we advance these studies further by linking the phenomenological study of aerosol-cloud-precipitation interactions in A-Train satellites to cloud lifetime effects. This allows us to use A-Train observations to constrain cloud lifetime effects of aerosols in global climate models.

2. Methods

[5] The probability of precipitation (POP) [*L'Ecuyer et al.*, 2009] and precipitation frequency susceptibility (S_{pop}) are constructed for warm (cloud top temperature > 273 K) marine clouds from nearly-coincident observations of aerosols, clouds and precipitation by the A-Train satellites. S_{pop} is

[1]Atmospheric Science and Global Change Division, Pacific Northwest National Laboratory, Richland, Washington, USA.
[2]Department of Atmospheric and Oceanic Sciences, University of Wisconsin, Madison, Wisconsin, USA.
[3]Mesoscale and Microscale Meteorology Division, National Center for Atmospheric Research, Boulder, Colorado, USA.
[4]Joint Institute for the Study of the Atmosphere and Ocean, University of Washington, Seattle, Washington, USA.
[5]Department of Atmospheric, Oceanic, and Space Sciences, University of Michigan, Ann Arbor, Michigan, USA.

Corresponding author: M. Wang, Atmospheric Science and Global Change Division, Pacific Northwest National Laboratory, Richland, WA 99354, USA. (Minghuai.Wang@pnnl.gov)

0094-8276/12/2012GL052204

defined as $-d\ln(POP)/d\ln(AI)$, where AI is the Aerosol Index (the product of aerosol optical depth (AOD) and Ångström coefficient) and is a proxy for column cloud condensation nuclei (CCN) concentration. The two measures (POP and S_{pop}) are then used to evaluate aerosol-cloud-precipitation interactions for warm marine clouds in two conventional aerosol-climate models, NCAR Community Atmosphere Model version 5 (CAM5) [*Liu et al.*, 2012; *Ghan et al.*, 2012] and ECHAM5-HAM2 [*Zhang et al.*, 2012], as well as in a multi-scale aerosol-climate model PNNL-MMF. The PNNL-MMF is based on the Multi-scale Modeling Framework (MMF) approach that explicitly treats aerosol effects on clouds using a cloud-resolving model (CRM) embedded within each grid cell of the host general circulation model (GCM) [*Wang et al.*, 2011b]. These models are briefly described in the auxiliary material.[1]

[6] The analysis of POP based on the A-Train observations has been documented in detail in *L'Ecuyer et al.* [2009] and is only briefly described here. POP is defined as the ratio of the number of precipitating events over the total number of cloudy events. POP is sorted into LWP bins as well as into different atmospheric stability conditions to isolate aerosol effects from atmospheric thermodynamics. Unstable environments are defined as having a lower tropospheric static stability (LTSS, defined as the difference in potential temperature between 700 hPa and the surface [*Klein and Hartmann*, 1993]) of less than 13.5 K, stable environments are defined as having a LTSS higher than 18.0 K and intermediate stable environments are defined as having a LTSS between 13.5 K and 18.0 K. Temperature and humidity profiles from ECMWF are used to estimate LTSS.

[7] Analysis of S_{pop} was not included in *L'Ecuyer et al.* [2009], but is performed here to quantify the dependence of POP on aerosol loading. Data are first sorted according to AI, and POP is calculated at 10 equally sampled AI bins. S_{pop} is then derived from the linear regression of ln(POP) vs. ln(AI).

[8] We used coincident daily observations of LWP at 12 km resolution from the AMSR-E, AOD and Ångström coefficient from $1^\circ \times 1^\circ$ MODIS data, and radar reflectivity from the CloudSat 2C-PRECIP-COLUMN dataset [*Haynes et al.*, 2009] at about 1.5 km resolution from 2007 to 2010 (see [*L'Ecuyer et al.*, 2009] for a more detailed description). For model results, daily output at the satellite overpass time (1:30 pm local time) are used. AI is from the output at the GCM grid (about 100 kilometers). For cloud fields, the MMF CRM results are based on the cloud-scale output on the grid of the embedded CRM (4-kilometer grid-spacing), while the MMF GCM results, as well as CAM5, ECHAM5-HAM2 results are based on the output on the GCM grids, and in-cloud LWP and surface rain rate from the GCM grid column are used. For the MMF GCM, CAM5, and ECHAM5-HAM2 results, the number of precipitating events and the number of cloudy events are weighted by the GCM grid column output for cloud fraction. The sampling is limited to 60°S to 60°N. The 'rain certain' category is used to define a rain event. Here, 'rain certain' is attenuation-corrected near surface radar reflectivity in excess of 0 dBZ in A-Train observations and surface precipitation rate above 0.6 mm/day in models (see Figure S1 and a discussion of the consistency between these two definitions in the auxiliary material).

3. Results

[9] Figure 1 shows POP as a function of LWP for high and low aerosol loading in marine clouds from the A-Train observations and PD simulations of two models: MMF and CAM5. The POP dependence on LWP and atmospheric stability from the A-Train observations has been documented in detail in *L'Ecuyer et al.* [2009]. Here we focus on dependence of POP on aerosol loading. The A-Train observations show smaller POP at high AI than at low AI, suggesting a suppression of precipitation occurrence at high AI [*L'Ecuyer et al.*, 2009]. The MMF CRM results (Figure 1b) also produce higher POP for lower AI, although the difference in POP between the high AI and low AI in MMF is larger than observed. The MMF GCM results (Figure 1c) also produce a separation in POP between the high AI and low AI cases. In contrast, CAM5 produces a much larger difference in POP between high and low aerosol loadings than in the observations and MMF. S_{pop} from the A-Train observations is small, less than 0.2 at all LWP values (Figure 2a), while S_{pop} is substantially larger in both MMF (Figure 2b, based on the MMF CRM results) and CAM5 (Figure 2c). The LWP-weighted (mean) S_{pop} is 0.12, 0.38, and 0.95 for satellite, MMF and CAM5, respectively.

[10] The larger S_{pop} in CAM5 than in MMF is consistent with the previously documented stronger LWP response to CCN perturbation in CAM5 [*Wang et al.*, 2011a]. This suggests that S_{pop} can be used as a measure of the LWP response to CCN perturbations in global climate models. To further test this idea, Figure 3a shows a scatter plot of the LWP-weighted S_{pop} from PD simulations and the global mean LWP response to CCN perturbations ($\lambda = d\ln(LWP)/d\ln(CCN)$) for marine clouds from three models: MMF, CAM5, and ECHAM5-HAM2. λ is calculated from the global annual-mean grid-average LWP (cloud fraction times in-cloud LWP) and CCN over ocean from PD and PI simulations and represents the model cloud lifetime effect of anthropogenic aerosols. Also included are 17 CAM5 sensitivity tests with different formulas for the autoconversion process (the initial generation of raindrops from cloud droplet collision and coalescence) (See Table S1 of the auxiliary material for a detailed description of the sensitivity tests). These sensitivity tests include different minimum cloud droplet number concentrations in the autoconversion formula (A-D), different autoconversion formulas (A-K from [*Khairoutdinov and Kogan*, 2000]; L-O from [*Chen and Cotton*, 1987]; and P-Q from [*Liu and Daum*, 2004]), different scaling factors for autoconversion rates (A, E, and F; G and H; N and O), different dependence of autoconversion rate on droplet number concentrations (G-Q), and different critical droplet effective radius (L-O). Since rain formation initiated through autoconversion can strongly depend on cloud droplet number concentration and therefore on aerosol burden, parameterization of the autoconversion process has been shown to play a critical role in determining the cloud

[1]Auxiliary materials are available in the HTML. doi:10.1029/2012GL052204.

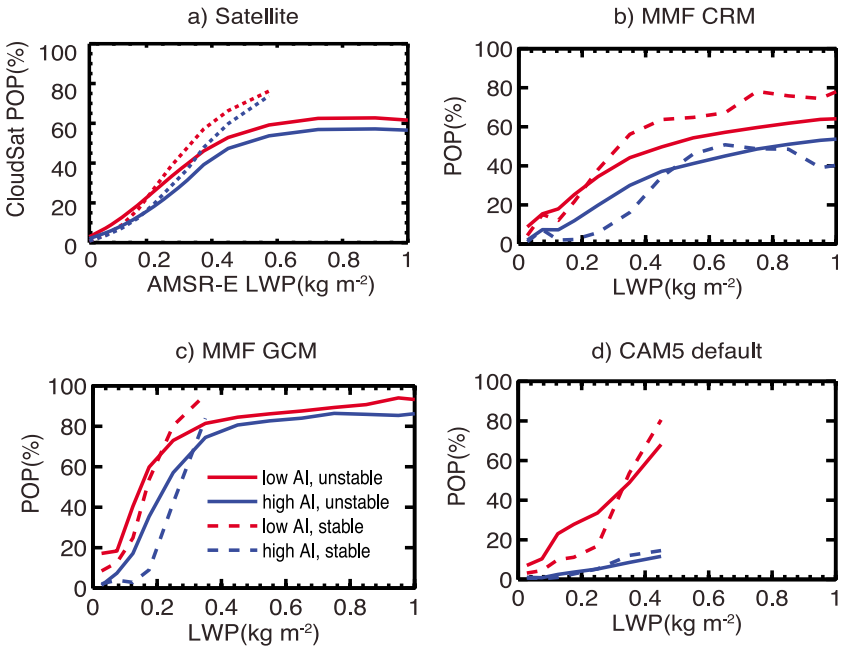

Figure 1. The probability of precipitation (POP) as a function of LWP (a) from the satellite observations; (b) from the MMF model using the CRM-scale output; (c) from the MMF model using the GCM-scale output; (d) from the default CAM5 with the GCM-scale output. Both satellite and model data are stratified by LTSS (stable: >18 K; and unstable: <13.5 K) and by AI (high AI: the highest 20 percentile; low AI: the lowest 20 percentile). The 'rain certain' category is used to define a 'rain' event (see text for details).

lifetime effect of aerosols in GCMs [e.g., *Penner et al.*, 2006].

[11] Figure 3a shows that λ and S_{pop} in these model experiments are strongly correlated with a correlation coefficient of 0.89. When the 'drizzle' category (radar reflectivity in excess of −15 dBZ in A-Train observations and surface precipitation rate above 0.12 mm/day in models) instead of the 'rain certain' category is used to define a rain event, λ and S_{pop} are still strongly correlated, but with a smaller correlation coefficient of 0.71 (Figure S2 of the auxiliary material).

[12] The strong correlation between λ and S_{pop} can be explained by the fact that both λ and S_{pop} in different model experiments are closely related to the magnitude of the autoconversion rate as shown in Figure 3b and Figure S3 of the auxiliary material. λ is strongly correlated with the ratio of the global mean vertically-integrated autoconversion rate and the global mean large-scale surface precipitation rate (AUTO/PRECL), with a correlation coefficient of 0.84 (Figure 3b). The one exception is case H, in which the autoconversion rate is independent of droplet number concentration (discussed further below). This correlation suggests that the magnitude of the autoconversion rate is important in determining the LWP response to CCN perturbation, which is consistent with previous studies [*Penner et al.*, 2006; *Rotstayn and Liu*, 2005]. Similarly, the correlation coefficient between AUTO/PRECL and S_{pop} is also strong, 0.76 (Figure S3 of the auxiliary material). We note that precipitation occurrence is closely related to the autoconversion process, since autoconversion must be sufficiently active in order for warm clouds to precipitate. In contrast, the precipitation *rate* is strongly dependent upon the accretion process [*Wood*, 2005], which is the growth of existing raindrops by collection of cloud droplets. The relative balance of autoconversion and accretion is critical for cloud lifetime effects of aerosols because accretion has little dependence on cloud droplet concentration and hence

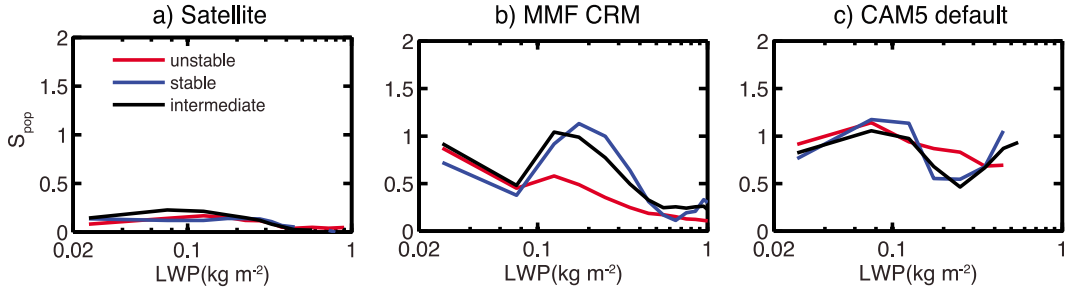

Figure 2. The precipitation frequency susceptibility (S_{pop}) as a function of LWP from both satellite observations and models: (a) from the satellite observations; (b) from the MMF model with the CRM-scale output; (c) from the default CAM5 with the GCM-scale output.

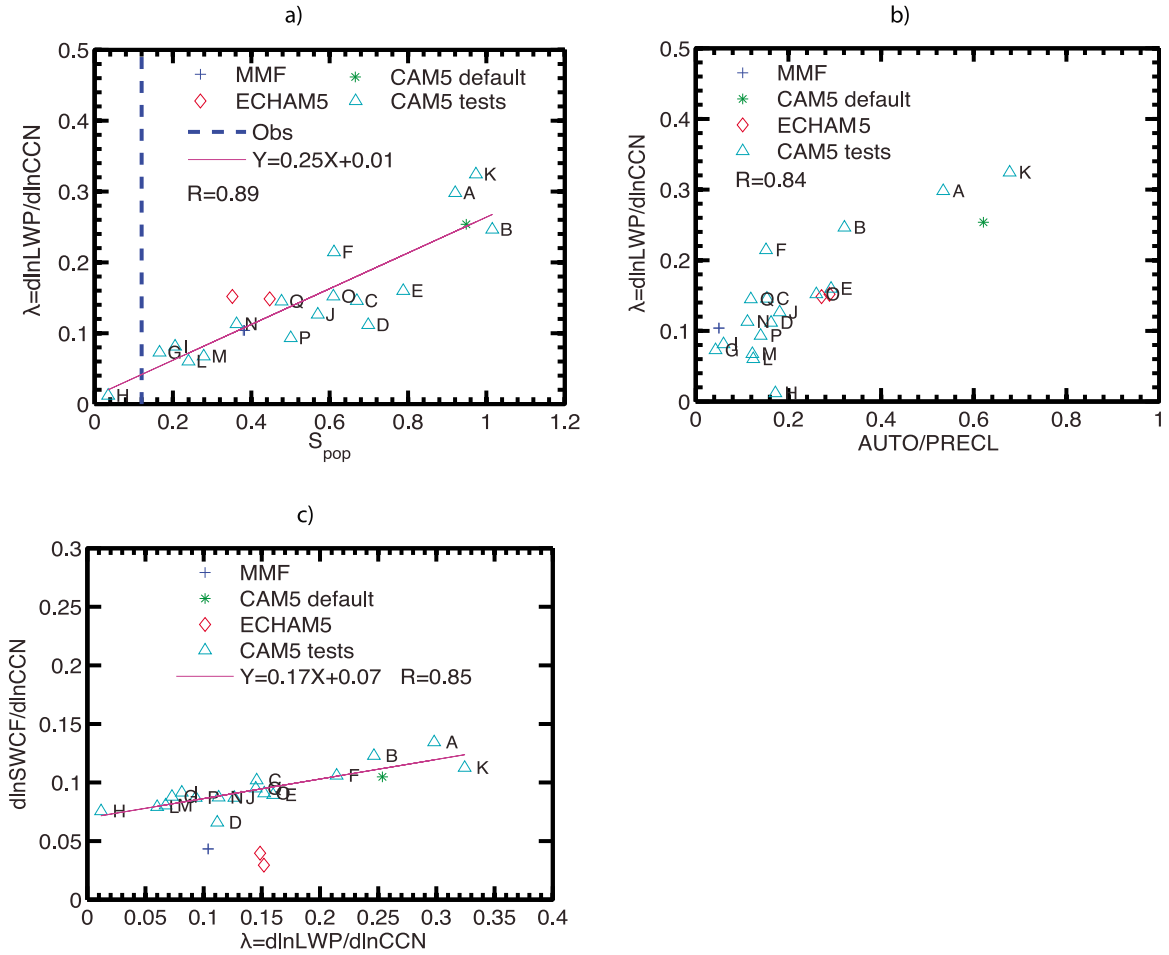

Figure 3. (a) The scatter plot of S_{pop} vs. λ for marine clouds from three different models: MMF (pluses), ECHAM5 (diamonds), and CAM5 in the default (asterisk), and sensitivity tests (triangles with symbols, see Table S1 of the auxiliary material for the details). For MMF, S_{pop} is calculated from both the CRM-scale output and the GCM-scale output, and as they are almost identical, only one plus symbol is shown. For ECHAM5, results from coarse (T42, left) and fine (T63, right) resolutions are shown. Averaged CCN concentrations (at 0.1% supersaturation) from surface to about 800 hPa are used to calculate λ. The solid line, equation and the correlation coefficient ('R') are from the linear fitting between λ and S_{pop} from all model experiments. The dashed line indicates S_{pop} from satellite observations. (b) The scatter plot of λ vs. the ratio of the annual mean vertically-integrated autoconversion rate over ocean to the annual mean surface precipitation rate from large-scale clouds over ocean (AUTO/PRECL) from all model experiments. For ECHAM5, results from coarse (T42, right) and fine (T63, left) resolutions are shown. (c) The scatter plot of $d\ln(\mathrm{SWCF})/d\ln(\mathrm{CCN})$ vs. λ for all model experiments. Here the solid line, equation and the correlation coefficient are from the linear fitting between $d\ln(\mathrm{SWCF})/d\ln(\mathrm{CCN})$ and λ for CAM5 experiments only. For ECHAM5, results from coarse (T42, bottom) and fine (T63, top) resolutions are shown.

aerosols in contrast to autoconversion [*Posselt and Lohmann*, 2009].

[13] The AUTO/PRECL ratios are 0.3 and 0.6 in ECHAM5-HAM2 and CAM5, respectively. The ratio in the MMF is much smaller, only 0.05. The smaller ratio in the MMF can be partly explained by the use of a prognostic rain scheme in the MMF, while those used in CAM5 and ECHAM5-HAM2 are diagnostic. Diagnostic rain schemes can shift the rain production from the accretion process to the autoconversion process [*Posselt and Lohmann*, 2009]. The minor role of autoconversion in rain production in MMF is consistent with that estimated from field observations in stratiform boundary layer clouds [*Wood*, 2005]. By modifying the autoconversion parameterization in the CAM5 sensitivity experiments, the AUTO/PRECL ratio is as low as 0.05.

[14] Precipitation susceptibility is a similar metric recently used to quantify cloud-aerosol-precipitation interactions. In its original definition [e.g., *Sorooshian et al.*, 2009], precipitation susceptibility (S_R) is calculated using the surface precipitation rate (R) instead of POP. Since S_R depends on precipitation rate, unlike POP, it is strongly influenced by the accretion process. S_R calculated from the MMF shows strong dependence on many non-microphysical factors, and is not able to constrain the dependence of the autoconversion rate on cloud droplet number concentration (Figure S4 and the detailed discussion in the auxiliary material). Furthermore, unlike S_R, aerosol effects on delaying the onset of precipitation are taken into account in S_{pop} since it includes non-precipitating events. It is also easier to derive S_{pop} from the A-Train observations, as it is much easier to distinguish a

raining cloud from a non-raining cloud with CloudSat than to provide an accurate measure of surface precipitation rate [*Haynes et al.*, 2009]. We note that a modified precipitation susceptibility formula (S_{POPxR}) introduced by *Terai et al.* [2012] was calculated using the product of rain rate and precipitation frequency. Further work is needed to quantify whether this new metric can be used to constrain cloud lifetime effects.

[15] Given the robust relationship between S_{pop} and λ found among all the models, the substantially smaller S_{pop} in the A-Train observations suggests that the LWP response to CCN perturbations in global climate models is overestimated. A linear fit between S_{pop} and λ from different model experiments in Figure 3a results in the following equation:

$$\lambda = 0.25 S_{pop} + 0.01. \quad (1)$$

[16] The value of S_{pop} from the A-Train observations (0.12) produces a λ of 0.04. When the drizzling category is used instead of the 'rain certain' category, the λ derived from the A-Train observations is slightly smaller (0.03) (Figure S2 of the auxiliary material). The smaller λ implied by the A-Train observations is consistent with ship track observations [e.g., *Coakley and Walsh*, 2002] and cloud-resolving model studies [e.g., *Ackerman et al.*, 2004].

4. Discussion

[17] Since the removal of aerosols by precipitation (wet scavenging) can lead to low aerosol loadings at high POP, wet scavenging can potentially bias S_{pop} high in both observations and models. However, our results show that the large differences in S_{pop} between A-Train observations and models are unlikely to be attributed to the wet scavenging effects in models. Cases H and G of the CAM5 sensitivity tests exclude aerosol effects on precipitation through autoconversion (autoconversion rate is independent of cloud droplet number concentration), but they include wet scavenging of aerosols. The LWP-weighted S_{pop} is 0.04 in case H and 0.17 in case G, much smaller than that in the CAM5 default experiment (0.98) (Figure 3a). We note that both λ and S_{pop} in case G are larger than in case H. This can be partly explained by the sedimentation effects of cloud droplets, either directly through its contribution to surface precipitation or indirectly through its effects on cloud water, radiation and dynamics. As the autoconversion rate in case G is one-tenth of that in case H, cloud droplet size is expected to be larger in case G, and therefore the sedimentation effects of cloud droplets are larger, which leads to larger λ and S_{pop}. This is demonstrated by an additional CAM5 sensitive test, which is identical to case G, except that the sedimentation of cloud droplets is turned off. In this test, λ and S_{pop} are reduced to 0.03 and 0.11, respectively. The remaining differences between H and G are likely explained by complex interactions between droplet size, radiation, microphysics, dynamics and LWP, as well as the precipitation scavenging of aerosols. The relatively small role played by wet scavenging on S_{pop} may be explained by the fact that POP is primarily determined by the initial phase of rain events, which typically have a small rain rate and hence limited scavenging. Furthermore, the aerosol fields used in both A-Train observations and models are averaged over a larger spatial scale than the cloud and precipitation fields (see Section 2), which also reduces precipitation effects on aerosol fields.

[18] *McComiskey and Feingold* [2012] examined the impact of data aggregation and the computational approach on statistical properties of the aerosol or cloud variables and their covariance. They demonstrated that the lack of a constraint on LWP can dampen the measured strength of the cloud albedo effect. In our study, both LWP and the atmospheric stability are used to constrain the data (see Section 2). Data aggregation can be another issue, though it is not clear whether this will increase or decrease the strength of aerosol-cloud-interactions as its impact depends on the heterogeneity of the aerosol and cloud properties and also the separation in space of aerosol and cloud properties from passive satellite remote sensors [*McComiskey and Feingold*, 2012]. In our analysis of A-Train observations, only aerosol products are aggregated up to the $1^\circ \times 1^\circ$ product, while cloud data (including both LWP and radar reflectivity) are not aggregated. This approach greatly increases the availability of coincident observations of aerosols, clouds, and precipitation, while at the same time reducing the impact of data aggregation since aerosol fields are more homogeneous than cloud fields [e.g., *McComiskey and Feingold*, 2012, Table 2]. The results from the MMF model also suggest that the effects of the data aggregation in determining S_{pop} appear to be small, as S_{pop} from the MMF CRM results (at 4-km horizontal grid-spacing) and from the MMF results (at about 100 kilometer grid-spacing) are quite similar (identical in Figure 3a and slightly different in Figure S2 of the auxiliary material). Nevertheless, uncertainties remain in satellite observations, such as the collocation of aerosol layers and cloud layers (column aerosol optical properties are used in both model and satellite analysis, and we do not distinguish whether aerosol and cloud layers are mixed or not), and cloud contamination of aerosol retrievals. More work is needed to further quantify the uncertainties in satellite derived S_{pop}.

[19] In this study, the strong correlation between S_{pop} and λ is derived based on three global climate models, and can be explained by the strong dependence of both S_{pop} and λ on the autoconversion process. Although autoconversion is the dominant process in determining cloud lifetime effects of aerosols in global climate models, there are many dynamical feedbacks involved in determining how LWP and cloud fraction respond to aerosol perturbations, such as sedimentation, evaporation cooling, and entrainment [e.g., *Ackerman et al.*, 2004]. Many of these feedbacks have not been incorporated into global climate models yet. A recently developed dynamical PDF cloud scheme shows some promise in incorporating such effects [*Guo et al.*, 2011]. More efforts are needed to examine how S_{pop} and λ are related using these advanced parameterizations and high-resolution models.

5. Implications

[20] The smaller λ derived from the A-Train observations would imply a substantially smaller shortwave aerosol indirect forcing than that estimated in GCMs. Figure 3c examines the relationship between the shortwave cloud forcing (SWCF) response to CCN perturbation ($d\ln(\text{SWCF})/d\ln(\text{CCN})$)

and λ over oceans in the different model experiments shown in Figure 3a. For the CAM5 experiments, the SWCF response to the CCN perturbation can be described well by a linear fit between $d\ln(\text{SWCF})/d\ln(\text{CCN})$ and λ: $d\ln(\text{SWCF})/d\ln(\text{CCN}) = 0.17\lambda + 0.07$. The intercept of the linear fit (0.07) is the cloud albedo effect, while 0.17λ is the cloud lifetime effect. A value of λ of 0.04 as implied by the A-Train observations gives a value for $d\ln(\text{SWCF})/d\ln(\text{CCN})$ of 0.077 in CAM5, and suggests a 33% reduction in the shortwave aerosol indirect forcing (defined as the differences in shortwave cloud forcing between PD and PI simulations, which is different from that used in [*Ghan et al.*, 2012]) from -1.56 W/m^2 in the default CAM5 to -1.04 W/m^2 over ocean. If we make the crude assumption that the dependence of the shortwave cloud forcing on LWP is similar in the three models, the same slope as that in CAM5 can be applied to MMF and ECHAM5-HAM2, and similar equations can be derived for ECHAM5-HAM2 and MMF but with different intercepts (0.015 for ECHAM5-HAM2, and 0.037 for MMF). This would lead to a 40% and 20% reduction in $d\ln(\text{SWCF})/d\ln(\text{CCN})$ in ECHAM5-HAM2 and MMF, respectively, if the value of λ of 0.04 implied by the A-Train observations is used.

[21] The smaller intercepts in MMF and ECHAM5-HAM2 than in CAM5 can likely be attributed to smaller cloud albedo effects in these two models than in CAM5. This is partly supported by the apparent deviation of case D from the regression line of the CAM5 experiments in Figure 3c. Unlike case C in which a minimum droplet number concentration of 20 cm^{-3} is only applied to the autoconversion process, the minimum droplet number concentration of 20 cm^{-3} in case D is also applied to the calculation of droplet effective radius used in the radiative transfer calculations. This leads to smaller cloud albedo effects and therefore leads to the deviation of case D from the regression line. The same minimum droplet number concentration of 20 cm^{-3} is applied to all physical processes in ECHAM5-HAM2, which may partly explain why this model has a smaller cloud albedo effect. Other differences among these models, such as the radiative transfer parameterization, the droplet effective radius, and vertical and horizontal cloud water distribution may also contribute to the different slopes. Further work is needed to test whether the strong linear relationship between $d\ln(\text{SWCF})/d\ln(\text{CCN})$ and λ in CAM5 is also found in other global climate models and can be used as a general method to separate cloud lifetime effects from cloud albedo effects.

[22] **Acknowledgments.** We thank Laura Riihimaki for her internal review. This work was supported by the NASA Interdisciplinary Science Program under grant NNX07AI56G and by the U.S. Department of Energy (DOE), Office of Science, Atmospheric System Research program, the Scientific Discovery through Advanced Computing (SciDAC) program, and the Decadal and Regional Climate Prediction using Earth System Models (EaSM) program. H.M. was supported by NOAA grant NA08OAR4310543, U.S. DOE ARM DE-FG02-08ER64574, and the NSF Science and Technology Center for Multiscale Modeling of Atmospheric Processes (CMMAP), managed by Colorado State University under cooperative agreement ATM-0425247. T.L. was supported under NASA grant NNX12AC51G. The Pacific Northwest National Laboratory (PNNL) is operated for the DOE by Battelle Memorial Institute under contract DE-AC06-76RLO 1830. We thank Paquita Zuidema for her careful review of the manuscript and constructive comments.

[23] The Editor thanks Paquita Zuidema for the assistance in evaluating this paper.

References

Ackerman, A. S., M. P. Kirkpatrick, D. E. Stevens, and O. B. Toon (2004), The impact of humidity above stratiform clouds on indirect aerosol climate forcing, *Nature*, *432*(7020), 1014–1017, doi:10.1038/nature03174.

Chen, C., and W. R. Cotton (1987), The physics of the marine stratocumulus-capped mixed layer, *J. Atmos. Sci.*, *44*(20), 2951–2977, doi:10.1175/1520-0469(1987)044<2951:TPOTMS>2.0.CO;2.

Coakley, J. A., and C. D. Walsh (2002), Limits to the aerosol indirect radiative effect derived from observations of ship tracks, *J. Atmos. Sci.*, *59*(3), 668–680, doi:10.1175/1520-0469(2002)059<0668:LTTAIR>2.0.CO;2.

Ghan, S. J., X. Liu, R. C. Easter, R. Zaveri, P. J. Rasch, J.-H. Yoon, and B. Eaton (2012), Toward a minimal representation of aerosols in climate models: Comparative decomposition of aerosol direct, semi-direct and indirect radiative forcing, *J. Clim.*, doi:10.1175/JCLI-D-11-00650.1, in press.

Guo, H., J. C. Golaz, and L. J. Donner (2011), Aerosol effects on stratocumulus water paths in a PDF-based parameterization, *Geophys. Res. Lett.*, *38*, L17808, doi:10.1029/2011GL048611.

Haynes, J. M., T. S. L'Ecuyer, G. L. Stephens, S. D. Miller, C. Mitrescu, N. B. Wood, and S. Tanelli (2009), Rainfall retrieval over the ocean with spaceborne W-band radar, *J. Geophys. Res.*, *114*, D00A22, doi:10.1029/2008JD009973.

Khairoutdinov, M., and Y. Kogan (2000), A new cloud physics parameterization in a large-eddy simulation model of marine stratocumulus, *Mon. Weather Rev.*, *128*(1), 229–243, doi:10.1175/1520-0493(2000)128<0229:ANCPPI>2.0.CO;2.

Klein, S. A., and D. L. Hartmann (1993), The seasonal cycle of low stratiform clouds, *J. Clim.*, *6*(8), 1587–1606, doi:10.1175/1520-0442(1993)006<1587:TSCOLS>2.0.CO;2.

Kubar, T. L., D. L. Hartmann, and R. Wood (2009), Understanding the importance of microphysics and macrophysics for warm rain in marine low clouds. Part I: Satellite observations, *J. Atmos. Sci.*, *66*(10), 2953–2972, doi:10.1175/2009JAS3071.1.

L'Ecuyer, T. S., and J. H. Jiang (2010), Touring the atmosphere aboard the A-Train, *Phys. Today*, *63*(7), 36–41, doi:10.1063/1.3463626.

L'Ecuyer, T. S., W. Berg, J. Haynes, M. Lebsock, and T. Takemura (2009), Global observations of aerosol impacts on precipitation occurrence in warm maritime clouds, *J. Geophys. Res.*, *114*, D09211, doi:10.1029/2008JD011273.

Leon, D. C., Z. Wang, and D. Liu (2008), Climatology of drizzle in marine boundary layer clouds based on 1 year of data from CloudSat and Cloud-Aerosol Lidar and Infrared Pathfinder Satellite Observations (CALIPSO), *J. Geophys. Res.*, *113*, D00A14, doi:10.1029/2008JD009835, [printed *114*(D8), 2009].

Liu, X., et al. (2012), Toward a minimal representation of aerosols in climate models: description and evaluation in the Community Atmospheric Model CAM5, *Geosci. Model Dev.*, *5*, 709–739, doi:10.5194/gmd-5-709-2012.

Liu, Y. G., and P. H. Daum (2004), Parameterization of the autoconversion process. Part I: Analytical formulation of the Kessler-type parameterizations, *J. Atmos. Sci.*, *61*(13), 1539–1548, doi:10.1175/1520-0469(2004)061<1539:POTAPI>2.0.CO;2.

Lohmann, U., and G. Lesins (2002), Stronger constraints on the anthropogenic indirect aerosol effect, *Science*, *298*(5595), 1012–1015, doi:10.1126/science.1075405.

Marshak, A., S. Platnick, T. Varnai, G. Y. Wen, and R. F. Cahalan (2006), Impact of three-dimensional radiative effects on satellite retrievals of cloud droplet sizes, *J. Geophys. Res.*, *111*, D09207, doi:10.1029/2005JD006686.

McComiskey, A., and G. Feingold (2012), The scale problem in quantifying aerosol indirect effects, *Atmos. Chem. Phys.*, *12*(2), 1031–1049, doi:10.5194/acp-12-1031-2012.

Penner, J. E., J. Quaas, T. Storelvmo, T. Takemura, O. Boucher, H. Guo, A. Kirkevag, J. E. Kristjansson, and O. Seland (2006), Model intercomparison of indirect aerosol effects, *Atmos. Chem. Phys.*, *6*, 3391–3405, doi:10.5194/acp-6-3391-2006.

Penner, J. E., L. Xu, and M. H. Wang (2011), Satellite methods underestimate indirect climate forcing by aerosols, *Proc. Natl. Acad. Sci. U. S. A.*, *108*(33), 13,404–13,408, doi:10.1073/pnas.1018526108.

Posselt, R., and U. Lohmann (2009), Sensitivity of the total anthropogenic aerosol effect to the treatment of rain in a global climate model, *Geophys. Res. Lett.*, *36*, L02805, doi:10.1029/2008GL035796.

Quaas, J., and O. Boucher (2005), Constraining the first aerosol indirect radiative forcing in the LMDZ GCM using POLDER and MODIS satellite data, *Geophys. Res. Lett.*, *32*, L17814, doi:10.1029/2005GL023850.

Quaas, J., O. Boucher, N. Bellouin, and S. Kinne (2008), Satellite-based estimate of the direct and indirect aerosol climate forcing, *J. Geophys. Res.*, *113*, D05204, doi:10.1029/2007JD008962.

Rotstayn, L. D., and Y. G. Liu (2005), A smaller global estimate of the second indirect aerosol effect, *Geophys. Res. Lett.*, *32*, L05708, doi:10.1029/2004GL021922.

Sorooshian, A., G. Feingold, M. D. Lebsock, H. L. Jiang, and G. L. Stephens (2009), On the precipitation susceptibility of clouds to aerosol perturbations, *Geophys. Res. Lett.*, *36*, L13803, doi:10.1029/2009GL038993.

Stephens, G. L., and J. M. Haynes (2007), Near global observations of the warm rain coalescence process, *Geophys. Res. Lett.*, *34*, L20805, doi:10.1029/2007GL030259.

Stephens, G. L., et al. (2002), The CloudSat mission and the A-Train: A new dimension of space-based observations of clouds and precipitation, *Bull. Am. Meteorol. Soc.*, *83*(12), 1771–1790, doi:10.1175/BAMS-83-12-1771.

Suzuki, K., T. Y. Nakajima, and G. L. Stephens (2010), Particle growth and drop collection efficiency of warm clouds as inferred from joint CloudSat and MODIS observations, *J. Atmos. Sci.*, *67*(9), 3019–3032, doi:10.1175/2010JAS3463.1.

Terai, C. R., R. Wood, D. C. Leon, and P. Zuidema (2012), Does precipitation susceptibility vary with increasing cloud thickness in marine stratocumulus?, *Atmos. Chem. Phys.*, *12*, 4567–4583, doi:10.5194/acp-12-4567-2012.

Wang, M., S. Ghan, M. Ovchinnikov, X. Liu, R. Easter, E. Kassianov, Y. Qian, and H. Morrison (2011a), Aerosol indirect effects in a multi-scale aerosol-climate model PNNL-MMF, *Atmos. Chem. Phys.*, *11*(11), 5431–5455, doi:10.5194/acp-11-5431-2011.

Wang, M., et al. (2011b), The multi-scale aerosol-climate model PNNL-MMF: model description and evaluation, *Geosci. Model Dev.*, *4*(1), 137–168, doi:10.5194/gmd-4-137-2011.

Wood, R. (2005), Drizzle in stratiform boundary layer clouds. Part II: Microphysical aspects, *J. Atmos. Sci.*, *62*(9), 3034–3050.

Zhang, K., et al. (2012), The global aerosol-climate model ECHAM-HAM, version 2: Sensitivity to improvements in process representations, *Atmos. Chem. Phys. Discuss.*, *12*(3), 7545–7615, doi:10.5194/acpd-12-7545-2012.